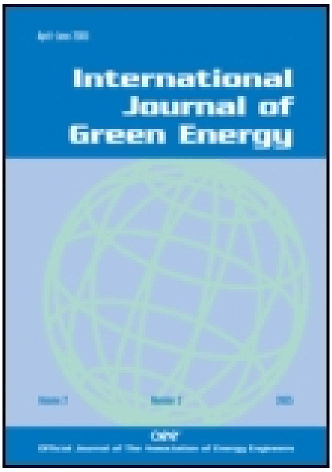

International Journal of Green Energy
Publication details, including instructions for authors and subscription information:
http://www.tandfonline.com/loi/ljge20

Solidification Characteristics Modeling of Phase Change Material in Plate Capsule of Cool Storage System

Guiyin Fang [a] & Zhi Chen [a]
[a] School of Physics, Jiangsu Province Engineering Research Center for New Refrigeration Technology , Nanjing University , Nanjing, 210093, China
Published online: 24 Oct 2011.

International Journal of Green Energy, 8: 734–747, 2011

ISSN: 1543-5075 print / 1543-5083 online
DOI: 10.1080/15435075.2011.602155

SOLIDIFICATION CHARACTERISTICS MODELING OF PHASE CHANGE MATERIAL IN PLATE CAPSULE OF COOL STORAGE SYSTEM

Guiyin Fang and Zhi Chen
School of Physics, Jiangsu Province Engineering Research Center for New Refrigeration Technology, Nanjing University, Nanjing 210093, China

The analytical solutions to solidification characteristics of a phase change material in the plate capsule of a cool storage system are presented. The influence of the Stefan number (the ratio of sensible heat to latent heat of a cool storage material) on phase change solidification thickness and temperature distribution in the solid region is analyzed. The phase change solidification thickness and temperature distribution in the solid region with second-order accuracy solutions are compared with those with first-order accuracy solutions for different Stefan numbers. It is found that the difference in temperature distribution in the solid region between second-order accuracy solutions and first-order accuracy solutions is very small as the Stefan number is small (i.e., Ste ≤ 0.1). In addition, the results present that the difference in phase change solidification thickness between second-order accuracy solutions and first-order accuracy solutions is small as the Stefan number is small (i.e., Ste ≤ 0.1). The phase change solidification thickness can be calculated using second-order accuracy solutions to obtain accurate calculation results as the Stefan number is large (i.e., Ste ≥ 0.1).

Keywords: ***Solidification characteristics; Heat transfer; Phase change material; Plate capsule; Cool storage***

INTRODUCTION

Cool storage systems are widely used in various industrial applications, such as food and chemical processing, where large short-duration loads are often required. The thermal energy stored for a long time is released in a short period of time and hence amplifies the cooling heat flux. A cool storage system plays a significant role in conserving available energy and improving its utilization. It is classified into two types: a sensible heat cool storage system and a latent heat cool storage system. The advantages of the latent heat cool storage system in comparison with the sensible heat cool storage system are high heat storage density, small size of the system, and a small temperature change during cool storage and release processes (Farid et al. 2004; Regin, Solanki, and Saini 2008). The most

Address correspondence to Guiyin Fang, School of Physics, Jiangsu Province Engineering Research Center for New Refrigeration Technology, Nanjing University, Nanjing 210093, China. E-mail: gyfang@nju.edu.cn

commonly used latent heat cool storage system is the encapsulated phase change materials (PCM) system, which uses a rectangular or cylindrical tank with plate or spherical capsules. PCMs can be grouped into two categories, namely organic and inorganic PCM.

During the solidification process, the position of the solid–liquid interface in the capsule continuously moves inward, and the penetration rate of the interface continuously changes. A phase change thermal energy storage system with spherical capsules was developed by Bedecarrats et al. (1996). Ismail and Henriquez (2000) presented a numerical study on PCM enclosed in a spherical capsule. The mathematical model was used to predict the effect of the size of the spherical capsule, shell thickness, material, initial temperature of the PCM and the external wall temperature on the solidified mass fraction and on the time for complete solidification. Ismail and Jesus (2001) conducted a parametric study on the solidification of a PCM in a cylinder carrying a heat transfer fluid inside. The results for the temperature distribution during the process, phase change interface velocity and thermal energy stored in the system were also presented. Ryu et al. (1991) used a rectangular storage tank with a copper-tube container and conducted a series of experiments to investigate the heat transfer characteristics. Cho and Choi (2000) investigated thermal characteristics of paraffin in a spherical capsule during freezing and melting processes. Kousksou et al. (2007) developed a theoretical model for analysis and optimization of a solar system with a cylindrical tank that contained spherical capsules filled with PCM. Energy and exergy analyses were carried out to understand the behavior of the system using single or multiple PCMs. Akgun, Aydm, and Kaygusuz (2008) experimentally studied the latent heat thermal energy storage system of the shell-and-tube type. Three kinds of paraffin with different melting temperatures were used as PCMs. The effects of the Reynolds and the Stefan number on the melting and solidification behaviors were determined. Cheralathan, Velraj, and Renganrayanan (2007) developed a simulation program to evaluate the temperature profiles of a heat transfer fluid and PCM at any axial location and studied the influence of the inlet temperature and porosity during the charging process. Eames and Adref (2002) described the results of an experimental study aimed at the characterization of the freezing and melting processes for water contained in spherical elements and developed semi-empirical equations. Kalaiselvam et al. (2008) studied the phase change behavior and heat transfer characteristics of PCM inside a spherical capsule used in tank, wherein *n*-tetradecane was used as a PCM.

This paper presents the analytical solutions to solidification characteristics of PCM in the plate capsule of a cool storage system. The influence of the Stefan number on phase change solidification thickness and temperature distribution in the solid region is analyzed. The phase change solidification thickness and temperature distribution in the solid region with second-order accuracy solutions are compared with those with first-order accuracy solutions for different Stefan numbers.

MATHEMATICAL MODEL AND METHOD OF SOLUTION

Figure 1 illustrates the schematic diagram of a cool storage system. The cool storage tank is a rectangular tank filled with stacked plate capsules is shown in Figure 2. The flat-plate capsules are stacked on top of each other with spacing in between successive capsules in order to provide flow channels for the heat transfer fluid. The PCM is sealed in the plate capsules. A coolant flows over the external wall of the plate capsules through the tank. The region of interest for this analysis is the control volume in a flat-plate capsule, as shown in Figure 3.

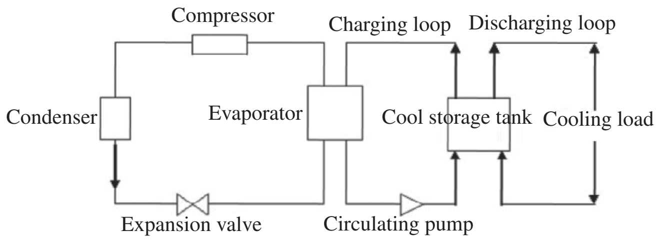

Figure 1 Schematic diagram of cool storage system.

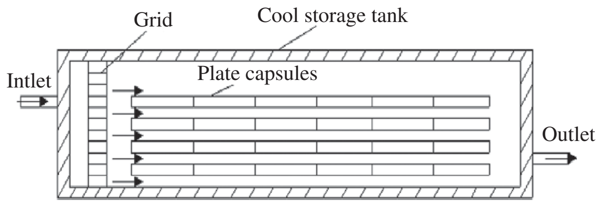

Figure 2 Schematic diagram of cool storage tank.

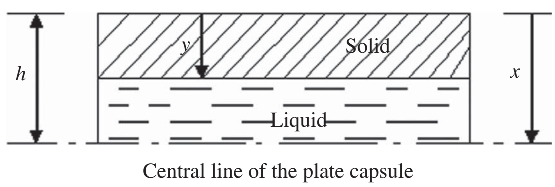

Figure 3 Schematic diagram of physical model in flat-plate capsule.

For a mathematical description, the following assumptions are made: (1) All thermophysical properties are constant. (2) The phase change heat transfer process occurs in the transitional zone between the solid–liquid interface. The temperature of the solid–liquid interface is unchangeable. (3) In this model, the boundary condition is considered to be the constant wall temperature. (4) The initial temperature in the capsule is equal to the PCM solidification temperature. (5) Because the capsule thickness is much smaller than its length and width, one-dimensional heat conduction along the thickness direction is considered. (6) During the solidification process, since interface movement velocity is much slower than temperature movement velocity, the temperature in the solid region is assumed to have a quasi-stable distribution (Chen 1991).

Referring to the physical model in Figure 3 (Fang and Li 2002), the governing equations for the solid region and the liquid region in the flat-plate capsule are as follows:

$$\rho_s c_s \frac{\partial T_s}{\partial t} = k_s \frac{\partial^2 T_s}{\partial x^2}, \text{for } 0 \le x < y; \tag{1}$$

$$\rho_l c_l \frac{\partial T_l}{\partial t} = k_l \frac{\partial^2 T_l}{\partial x^2}, \text{for } y < x \le h. \tag{2}$$

The boundary conditions are given by:

$$T_s = T_b, \text{at } x = 0; \tag{3}$$

$$\frac{\partial T_l}{\partial x} = 0, \text{at } x = h. \tag{4}$$

The initial condition is

$$T_l(x, 0) = T_m, \text{at } t = 0. \tag{5}$$

The solid–liquid interface conditions are

$$T_s = T_l = T_m, \text{at } x = y; \tag{6}$$

$$\rho_s H_s \frac{\partial y}{\partial t} = k_s \frac{\partial T_s}{\partial x}\Big|_y - k_l \frac{\partial T_l}{\partial x}\Big|_y, \text{at } x = y. \tag{7}$$

The following non-dimensional quantities are introduced:

$$\theta = \frac{T - T_b}{T_m - T_b}, X = \frac{x}{h}, S = \frac{y}{h}, \tau = \frac{\alpha_s t}{h^2} = \frac{k_s t}{\rho_s c_s h^2}, \text{ Ste} = \frac{c_s(T_m - T_b)}{H_s}.$$

The Stefan number is a dimensionless number that presents the ratio of sensible heat to latent heat of a cool storage material.

The following equations are obtained by substituting these quantities into Equations (1)–(7):

$$\frac{\partial^2 \theta_s}{\partial X^2} = \frac{\partial \theta_s(X, \tau)}{\partial \tau}, \text{for } 0 \le X < S, \tag{8}$$

$$\frac{\partial^2 \theta_l}{\partial X^2} = \frac{\alpha_s}{\alpha_l} \cdot \frac{\partial \theta_l(X, \tau)}{\partial \tau}, \text{for } S < X \le 1. \tag{9}$$

The boundary conditions are

$$\theta_s = 0, \text{at } X = 0, \tag{10}$$

$$\frac{\partial \theta_l}{\partial X} = 0, \text{at } X = 1. \tag{11}$$

The initial condition is

$$\theta_l = 1, \text{at } \tau = 0. \tag{12}$$

The solid–liquid interface conditions are

$$\theta_s = \theta_l = 1, \text{at } X = S, \tag{13}$$

$$\frac{1}{\text{Ste}} \frac{\partial S}{\partial \tau} = \frac{\partial \theta_s}{\partial X} - \frac{k_l}{k_s} \frac{\partial \theta_l}{\partial X}, \text{at } X = S. \tag{14}$$

The following equations are obtained by integrating Equations (8) and (9):

$$\int_0^s \frac{\partial \theta_s}{\partial \tau} dX = \int_0^s \frac{\partial^2 \theta_s}{\partial X^2} dX = \left.\frac{\partial \theta_s}{\partial X}\right|_s - \left.\frac{\partial \theta_s}{\partial X}\right|_0, \tag{15}$$

$$\int_s^1 \frac{\alpha_s}{\alpha_l} \frac{\partial \theta_l}{\partial \tau} dX = \int_s^1 \frac{\partial^2 \theta_l}{\partial X^2} dX = \left.\frac{\partial \theta_l}{\partial X}\right|_1 - \left.\frac{\partial \theta_l}{\partial X}\right|_s. \tag{16}$$

From Equations (15) and (16), one has:

$$\left.\frac{\partial \theta_s}{\partial X}\right|_s = \int_0^s \frac{\partial \theta_s}{\partial \tau} dX + \left.\frac{\partial \theta_s}{\partial X}\right|_0, \tag{17}$$

$$\left.\frac{\partial \theta_l}{\partial X}\right|_s = \left.\frac{\partial \theta_l}{\partial X}\right|_1 - \int_s^1 \frac{\alpha_s}{\alpha_l} \frac{\partial \theta_l}{\partial \tau} dX = -\int_s^1 \frac{\alpha_s}{\alpha_l} \frac{\partial \theta_l}{\partial \tau} dX. \tag{18}$$

Substituting Equations (17) and (18) into Equation (14), one gets:

$$\frac{1}{\mathrm{Ste}} \frac{\partial S}{\partial \tau} = \int_0^s \frac{\partial \theta_s}{\partial \tau} dX + \left.\frac{\partial \theta_s}{\partial X}\right|_0 + \frac{\rho_l c_l}{\rho_s c_s} \int_s^1 \frac{\partial \theta_l}{\partial \tau} dX. \tag{19}$$

By using the relation of $\frac{\partial \theta}{\partial \tau} = \frac{\partial \theta}{\partial S} \cdot \frac{\partial S}{\partial \tau}$, Equation (19) may be written as:

$$\frac{1}{\mathrm{Ste}} \frac{\partial S}{\partial \tau} = \left[\int_0^s \frac{\partial \theta_s}{\partial S} dX + \frac{\rho_l c_l}{\rho_s c_s} \int_s^1 \frac{\partial \theta_l}{\partial S} dX\right] \frac{\partial S}{\partial \tau} + \left.\frac{\partial \theta_s}{\partial X}\right|_0, \tag{19a}$$

$$\frac{\partial S}{\partial \tau} \left[\frac{1}{\mathrm{Ste}} - \int_0^s \frac{\partial \theta_s}{\partial S} dX - \frac{\rho_l c_l}{\rho_s c_s} \int_s^1 \frac{\partial \theta_l}{\partial S} dX\right] = \left.\frac{\partial \theta_s}{\partial X}\right|_0. \tag{19b}$$

According to assumption (5), wherein temperature distribution in the solid region in the flat-plate capsule is considered to be linear, one gets:

$$\theta_s = a_0 + a_1 X. \tag{20}$$

The following expression is obtained from Equation (20) for the temperature distribution at $X = 0$, $\theta_s = 0$ and $X = S$, $\theta_s = 1$:

$$\theta_s = \frac{X}{S}. \tag{21}$$

From Equation (21), one has:

$$\left.\frac{\partial \theta_s}{\partial X}\right|_0 = \frac{1}{S}, \tag{22}$$

$$\frac{\partial \theta_s}{\partial S} = -\frac{X}{S^2}. \tag{23}$$

In terms of the preceding assumption, the temperature profile of the liquid is given by the following expression:

$$T_\mathrm{l} = T_\mathrm{m}. \tag{24}$$

By non-dimensionalizing Equation (24), one obtains:

$$\theta_\mathrm{l} = 1. \tag{24a}$$

From Equation (24a), one has:

$$\frac{\partial \theta_\mathrm{l}}{\partial S} = 0. \tag{25}$$

From Equations (23) and (25), one gets:

$$\int_0^\mathrm{s} \frac{\partial \theta_\mathrm{s}}{\partial S} dX = -\frac{1}{2}, \tag{26}$$

$$\int_\mathrm{s}^1 \frac{\partial \theta_\mathrm{l}}{\partial S} dX = 0. \tag{27}$$

Substituting Equations (22), (26), and (27) into Equation (19b), one obtains:

$$\frac{\partial S}{\partial \tau} = \frac{2\mathrm{Ste}}{(2 + \mathrm{Ste}) \cdot S}. \tag{28}$$

Integrating Equation (28), one has:

$$S = \sqrt{\frac{4\mathrm{Ste}}{2 + \mathrm{Ste}}} \cdot \tau^{\frac{1}{2}} = 2\left(\frac{\mathrm{Ste}}{2 + \mathrm{Ste}} \cdot \tau\right)^{\frac{1}{2}}. \tag{29}$$

From the preceding calculation, one knows that the method of solution is simple with first-order accuracy. Now, when the temperature distribution in the solid region is assumed to be a polynomial, one gets:

$$\theta_\mathrm{s} = b_0 + b_1 X + b_2 X^2. \tag{30}$$

According to the boundary conditions $X = 0$, $\theta_\mathrm{s} = 0$ and $X = S$, $\theta_\mathrm{s} = 1$, the following equations are obtained from Equation (30):

$$b_0 = 0, \tag{31}$$

$$b_1 S + b_2 S^2 = 1. \tag{32}$$

From Equation (14), one obtains:

$$\frac{1}{\mathrm{Ste}} \frac{\partial S}{\partial \tau} = b_1 + 2b_2 S. \tag{33}$$

Substituting Equation (28) into Equation (33), one gets:

$$b_1 S + 2b_2 S^2 = \frac{2}{2+\mathrm{Ste}}. \tag{34}$$

From Equations (32) and (34), one has:

$$b_1 = \frac{2(1+\mathrm{Ste})}{(2+\mathrm{Ste})} \cdot \frac{1}{S}, \tag{35}$$

$$b_2 = -\frac{\mathrm{Ste}}{(2+\mathrm{Ste})} \cdot \frac{1}{S^2}. \tag{36}$$

Substituting Equations (31), (35), and (36) into Equation (30), one obtains:

$$\theta_\mathrm{s} = \frac{2(1+\mathrm{Ste})}{(2+\mathrm{Ste})} \cdot \frac{X}{S} - \frac{\mathrm{Ste}}{(2+\mathrm{Ste})} \cdot \frac{X^2}{S^2}. \tag{37}$$

From Equation (37), one has:

$$\left.\frac{\partial \theta_\mathrm{s}}{\partial X}\right|_0 = \frac{2(1+\mathrm{Ste})}{(2+\mathrm{Ste}) \cdot S}, \tag{38}$$

$$\frac{\partial \theta_\mathrm{s}}{\partial S} = -\frac{2(1+\mathrm{Ste})}{(2+\mathrm{Ste})} \cdot \frac{X}{S^2} + \frac{2\mathrm{Ste}}{(2+\mathrm{Ste})} \cdot \frac{X^2}{S^3}. \tag{39}$$

Substituting Equations (38), (39), and (27) into Equation (19b), one gets:

$$\frac{\partial S}{\partial \tau} = \frac{(6\mathrm{Ste} + 6\mathrm{Ste}^2)}{(6 + 6\mathrm{Ste} + \mathrm{Ste}^2)} \cdot \frac{1}{S}. \tag{40}$$

Integrating Equation (40), one obtains:

$$S = \left(\frac{12\mathrm{Ste} + 12\mathrm{Ste}^2}{6 + 6\mathrm{Ste} + \mathrm{Ste}^2}\right)^{\frac{1}{2}} \cdot \tau^{\frac{1}{2}}. \tag{41}$$

When the solidification process is final, $S = 1$, one gets:

$$\tau_\mathrm{f} = \frac{6 + 6\mathrm{Ste} + \mathrm{Ste}^2}{12\mathrm{Ste} + 12\mathrm{Ste}^2} = \frac{1}{2\mathrm{Ste}} + \frac{\mathrm{Ste}}{12(1+\mathrm{Ste})}. \tag{42}$$

In order to obtain more accurate results, we may get the temperature distribution in the solid region with third-order accuracy solution on the basis of second-order accuracy results. Now, when the temperature distribution in the solid region with third-order accuracy solution is assumed to be a polynomial, one obtains:

$$\theta_\mathrm{s} = c_0 + c_1 X + c_2 X^2 + c_3 X^3. \tag{43}$$

According to the boundary conditions $X = 0$, $\theta_s = 0$ and $X = S$, $\theta_s = 1$, from Equation (43), one has:

$$c_0 = 0, \tag{44}$$

$$c_1 S + c_2 S^2 + c_3 S^3 = 1. \tag{45}$$

From Equations (38) and (43), one obtains:

$$c_1 = \frac{2(1+\mathrm{Ste})}{(2+\mathrm{Ste})} \cdot \frac{1}{S}. \tag{46}$$

From Equation (14), one gets:

$$\frac{1}{\mathrm{Ste}} \frac{\partial S}{\partial \tau} = c_1 + 2c_2 S + 3c_3 S^2. \tag{47}$$

Substituting Equation (40) into Equation (47), one has:

$$c_1 S + 2c_2 S^2 + 3c_3 S^3 = \frac{6 + 6\mathrm{Ste}}{6 + 6\mathrm{Ste} + \mathrm{Ste}^2}. \tag{48}$$

From Equations (45), (46), and (48), one obtains:

$$c_2 = -\frac{\mathrm{Ste}}{(2+\mathrm{Ste})} \cdot \frac{(24 + 36\mathrm{Ste} + 14\mathrm{Ste}^2 + \mathrm{Ste}^3)}{(12 + 18\mathrm{Ste} + 8\mathrm{Ste}^2 + \mathrm{Ste}^3)} \cdot \frac{1}{S^2}, \tag{49}$$

$$c_3 = \frac{\mathrm{Ste}}{(2+\mathrm{Ste})} \cdot \frac{(12 + 18\mathrm{Ste} + 6\mathrm{Ste}^2)}{(12 + 18\mathrm{Ste} + 8\mathrm{Ste}^2 + \mathrm{Ste}^3)} \cdot \frac{1}{S^3}. \tag{50}$$

Substituting Equations (44), (46), (49), and (50) into Equation (43), one gets:

$$\begin{aligned}\theta_s = &\frac{2(1+\mathrm{Ste})}{(2+\mathrm{Ste})} \cdot \frac{X}{S} - \frac{\mathrm{Ste}}{(2+\mathrm{Ste})} \cdot \frac{(24 + 36\mathrm{Ste} + 14\mathrm{Ste}^2 + \mathrm{Ste}^3)}{(12 + 18\mathrm{Ste} + 8\mathrm{Ste}^2 + \mathrm{Ste}^3)} \cdot \frac{X^2}{S^2} \\ &+ \frac{\mathrm{Ste}}{(2+\mathrm{Ste})} \cdot \frac{(12 + 18\mathrm{Ste} + 6\mathrm{Ste}^2)}{(12 + 18\mathrm{Ste} + 8\mathrm{Ste}^2 + \mathrm{Ste}^3)} \cdot \frac{X^3}{S^3}.\end{aligned} \tag{51}$$

From Equation (51), one obtains phase change solidification thickness with third-order accuracy solutions.

RESULTS AND DISCUSSION

Comparison of the Temperature Distribution in Solid Region and Phase Change Solidification Thickness

The temperature distribution in the solid region and the phase change solidification thickness in the flat-plate capsule for different Stefan numbers are calculated by using Equations (21), (29), (37), and (41). As shown in Figure 4, the temperature distribution in

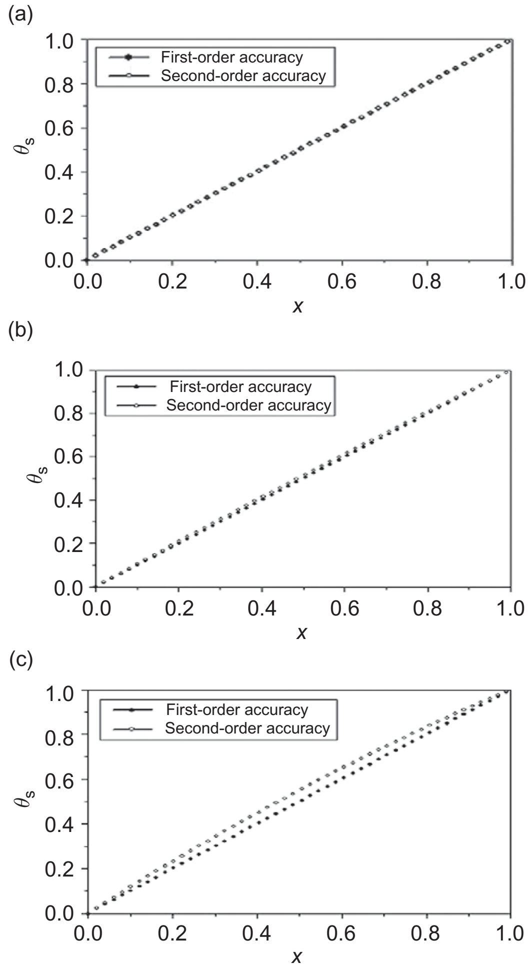

Figure 4 Temperature distribution in solid region at $S = 1$ and (a) Ste $= 0.01$, (b) Ste $= 0.1$, and (c) Ste $= 0.5$.

the solid region with second-order accuracy solutions is compared with that with first-order accuracy solutions at Ste $= 0.01$, Ste $= 0.1$, and Ste $= 0.5$. It is known that the difference in temperature distribution in the solid region between second-order accuracy solutions and first-order accuracy solutions is very small as the Stefan number is small (i.e., Ste ≤ 0.1). The temperature in the solid region can be calculated by using first-order accuracy solutions as Ste ≤ 0.1.

Figure 5 presents phase change solidification thickness with second-order accuracy solutions and first-order accuracy solutions at Ste $= 0.01$, Ste $= 0.1$, and Ste $= 0.5$. The results indicate that the difference in the phase change solidification thickness between second-order accuracy solutions and first-order accuracy solutions is small as the Stefan number is small (i.e., Ste ≤ 0.1). As Ste ≥ 0.1, the larger the dimensionless time τ, the larger the difference in the phase change solidification thickness between second-order accuracy solutions and first-order accuracy solutions. The phase change solidification thickness can be calculated by utilizing second-order accuracy solutions to obtain accurate calculation results as the Stefan number is large (i.e., Ste ≥ 0.1).

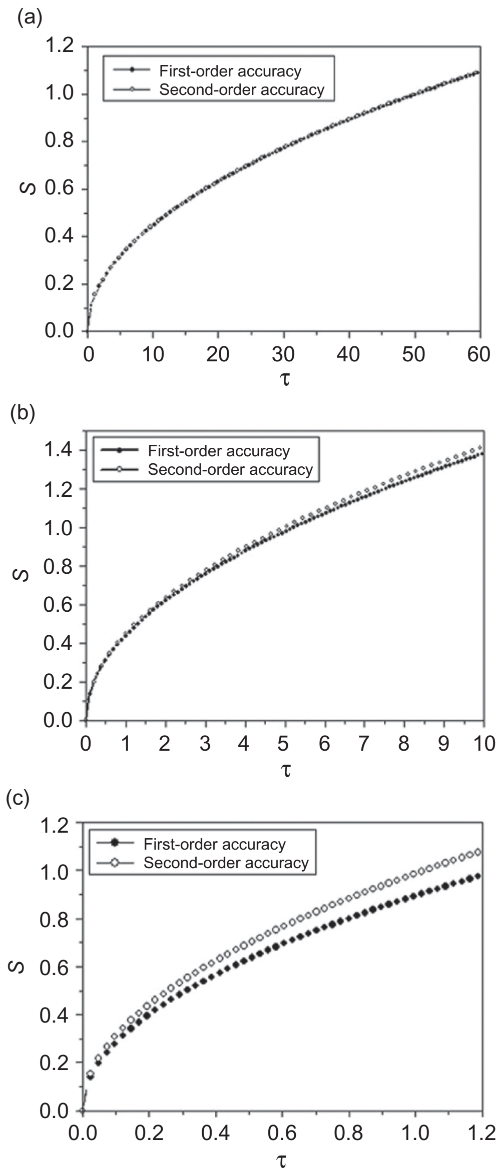

Figure 5 Phase change solidification thickness at (a) Ste $= 0.01$, (b) Ste $= 0.1$, and (c) Ste $= 0.5$.

Temperature Distribution in Solid Region and Phase Change Solidification Thickness with Second-Order Accuracy Solutions

Figure 6 shows the temperature distribution in the solid region with second-order accuracy solutions at $S = 0.5$ and $S = 1$. It can be observed from the figure that the temperature distribution in the solid region is approximately linear as Ste ≤ 0.1. The Stefan number has little influence on temperature distribution in the solid region for different solidification thicknesses. All temperature distributions approximately concentrate on a straight line and accord with a quasi-stable temperature distribution assumption.

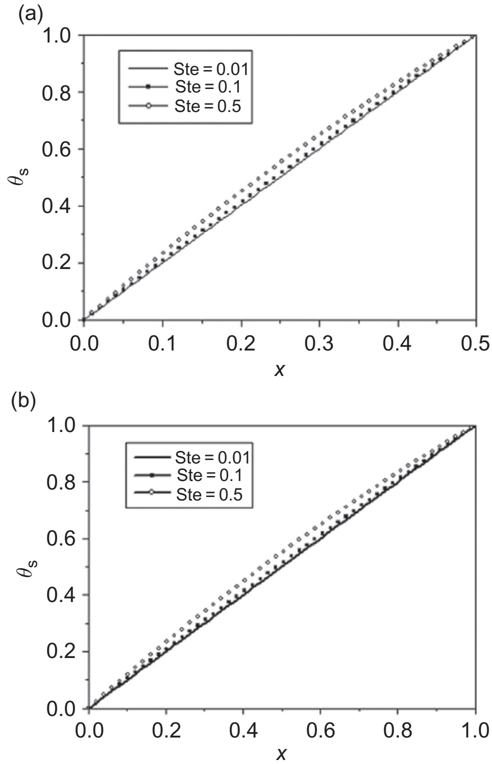

Figure 6 Temperature distribution in solid region with second-order accuracy solutions at (a) $S = 0.5$ and (b) $S = 1$.

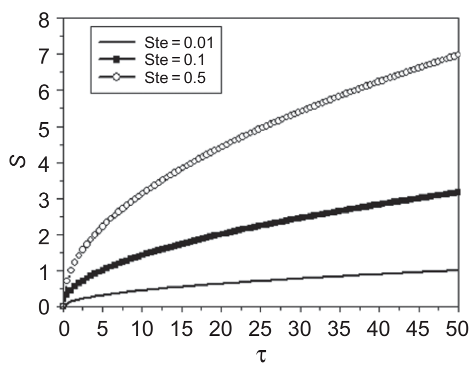

Figure 7 Phase change solidification thickness with second-order accuracy solutions.

Figure 7 presents the phase change solidification thickness with second-order accuracy solutions for Ste $= 0.01$, Ste $= 0.1$, and Ste $= 0.5$. It is known that the solidification thickness increases as the Stefan number increases. Thus, the Stefan number influences solidification thickness. The lower the wall temperature of the capsule, the larger the

Stefan number. The wall temperature is restricted by the coolant's temperature. As shown in Figure 7, the solidification thickness increases quickly during the initial cool storage period. This is due to the thinner solidification layer and the smaller thermal resistance during the initial period. It can also be observed from Figure 7 that the solidification rate varies with time. The solidification rate decreases when cool storage time increases. The larger the Stefan number, the larger the solidification rate.

CONCLUSIONS

This paper presents analytical solutions to solidification characteristics of PCM in the plate capsule for a cool storage system. The influence of the Stefan number (the ratio of sensible heat to latent heat of a cool storage material) on the phase change solidification thickness and temperature distribution in the solid region is discussed on the basis of analytical results. The conclusions acquired are as follows:

1. The difference in temperature distribution in the solid region between second-order accuracy solutions and first-order accuracy solutions is very small as Ste ≤ 0.1. The temperature in the solid region can be calculated by using first-order accuracy solutions as Ste ≤ 0.1 in a cool storage system.
2. The difference in phase change solidification thickness between second-order accuracy solutions and first-order accuracy solutions is small as the Stefan number is small (i.e., Ste ≤ 0.1). As Ste ≥ 0.1, the larger the dimensionless time τ, the larger the difference in solidification thickness between second-order accuracy solutions and first-order accuracy solutions. The solidification thickness can be calculated by utilizing second-order accuracy solutions to obtain accurate calculation results as the Stefan number is large (i.e., Ste ≥ 0.1).
3. The solidification thickness increases as the Stefan number increases, and increases quickly during the initial cool storage period. The large Stefan number benefits the solidification process, but it is restricted by the coolant's temperature.
4. This analytical method and the results can conveniently predict solidification characteristics of a flat-plate capsule of a cool storage system and provide useful calculation results for the design of the flat-plate capsule.

ACKNOWLEDGMENT

This project is supported by the National Natural Science Foundation of China (Grant no. 50776043), the Fundamental Research Funds for the Central Universities (Grant no. 1114020401), and the Priority Academic Program Development of Jiangsu Higher Education Institutions.

NOMENCLATURE

c (J/kg K)	Specific heat
H_s (J/kg)	Solidification latent heat of cool storage material
h (m)	Half thickness of the capsule
k (W/m K)	Thermal conductivity
S (–)	Dimensionless solidification thickness of cool storage material
Ste (–)	Stefan number

T (K) Temperature
t (s) Time
X (–) Dimensionless longitudinal coordinate
x (–) Longitudinal coordinate
y (m) Solidification thickness of cool storage material

Greek Letters

α (m^2/s) Thermal diffusivity
θ (–) Dimensionless temperature
ρ (kg/m^3) Density
τ (–) Dimensionless time

Subscripts

b (–) Wall of the capsule
l (–) Liquid cool storage material
m (–) Solidification point of cool storage material
s (–) Solid cool storage material

REFERENCES

Akgun, M., O. Aydm, and K. Kaygusuz. 2008. Thermal energy storage performance of paraffin in a novel tube-in-shell system. *Applied Thermal Engineering* 28:405–13.

Bedecarrats, J.P., F. Strub, B. Falcon, and J.P. Dumas. 1996. Phase change thermal energy storage using spherical capsules: Performance of a test plant. *International Journal of Refrigeration* 19:187–96.

Chen, Z.S. 1991. A simple heat resistance method for the solution to heat conduction undergoing solidification. *Journal of University of Science and Technology of China* 21(3):69–76.

Cheralathan, M., R. Velraj, and S. Renganrayanan. 2007. Effect of porosity and the inlet heat transfer fluid temperature variation on the performance of cool thermal energy storage system. *Heat Mass Transfer* 43:833–42.

Cho, K., and S.H. Choi. 2000. Thermal characteristics of paraffin in a spherical capsule during freezing and melting processes. *International Journal of Heat Mass & Transfer* 43:3183–96.

Eames, I.W., and K.T. Adref. 2002. Freezing and melting of water in spherical enclosures of the type used in thermal (ice) storage systems. *Applied Thermal Engineering* 22:733–45.

Fang, G.Y., and H. Li. 2002. Study on dynamic charging performance of ice storage of stacked rectangular capsules. *International Journal on Architectural Science* 3(4):135–41.

Farid, M.M., A.M. Khudhair, S.A.K. Razack, and S. Al-Hallaj. 2004. A review on phase change energy storage: Materials and applications. *Energy Conversation & Management* 45:1597–1615.

Ismail, K.A.R., and J.R. Henriquez. 2000. Solidification of PCM inside a spherical capsule. *Energy Conversation & Management* 41:173–87.

Ismail, K.A.R., and A.B.D. Jesus. 2001. Parametric study of solidification of PCM around a cylinder for ice-bank applications. *International Journal of Refrigeration* 24:809–22.

Kalaiselvam, S., M. Veerappan, A.A. Aaronb, and S. Iniyan. 2008. Experimental and analytical investigation of solidification and melting characteristics of PCMs inside cylindrical encapsulation. *International Journal of Thermal Sciences* 47:858–74.

Kousksou, T., F. Strub, J.C. Lasvignottes, A. Jamil, and J.P. Bedecarrats. 2007. Second law analysis of latent thermal storage for solar system. *Solar Energy Materials & Solar Cells* 91:1275–81.

Regin, A.F., S.C. Solanki, and J.S. Saini. 2008. Heat transfer characteristics of thermal energy storage system using PCM capsules: A review. *Renewable and Sustainable Energy Reviews* 12:2438–58.

Ryu, H.W., S.A. Hong, B.C. Shin, and S.D. Kim. 1991. Heat transfer characteristics of cool-thermal storage systems. *Energy* 16:727–37.